

1 **Supporting Information**

2 **Cryogenic Efficient Phase Separation of Oil-water**
3 **Emulsions with Amphiphilic Hyperbranched**
4 **Poly(amido-amine)**

5 *Shu Yan*^{a, c}, *Pengfei Jiang*^b, *Xinghong Zhang*^{a, c}, *Yongsheng Guo*^{b, c**},
6 *and Wenjun Fang*^{b, c*}

7 ^a Department of Polymer Science and Engineering, Zhejiang University, Hangzhou
8 310027, China

9 ^b Department of Chemistry, Zhejiang University, Hangzhou 310058, China

10 ^c Center of Chemistry for Frontier Technologies, Zhejiang University, Hangzhou
11 310027, China

12 * Corresponding author. Tel.: +86-571-88981416; Fax: +86-571-88981416

13 Email address: fwjun@zju.edu.cn

14

15

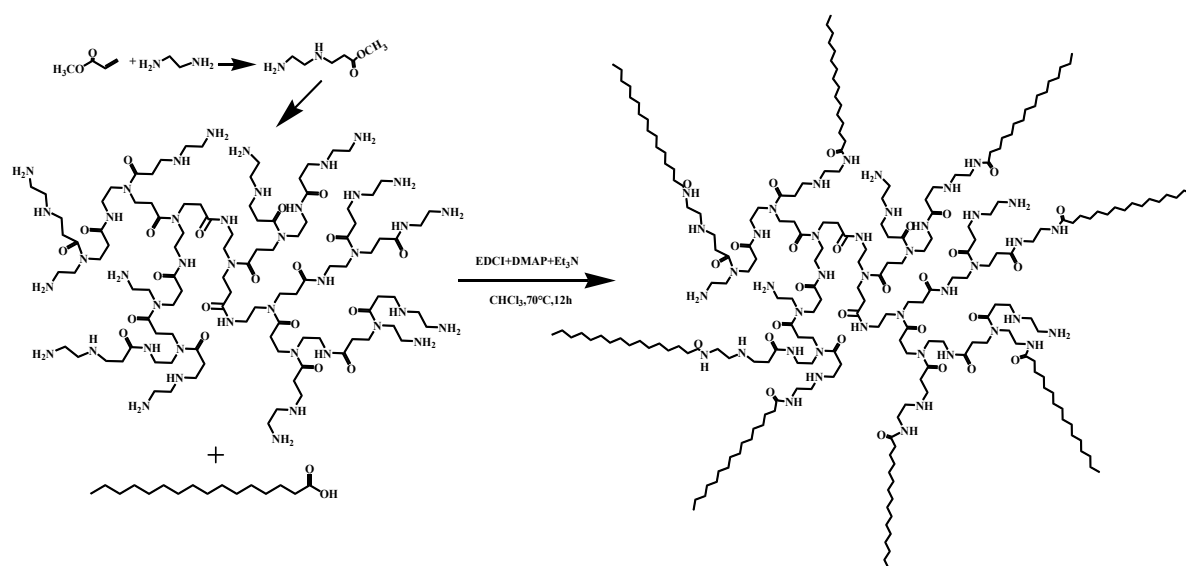
16 **I. Materials**

17 Ethylenediamine (EDA) (99 %), methyl acrylate (MA) (98.5 %), palmitic acid (97
18 %), Tween 80, Span 80, 4-dimethylaminopyridine (DMAP, 99 %) and 1-ethyl-3-(3-
19 dimethylaminopropyl) carbodiimide hydrochloride (EDCI, 98 %) were purchased
20 from Aladdin Chemical Reagent Corporation. Methanol (99.5 %), ethyl ether (99.5
21 %), chloroform (99 %), acetone (99.5 %), toluene (99.5 %), *n*-hexane (97 %), and
22 triethylamine (Et₃N, 99 %) were purchased from Sino-pharm Chemical Reagent

23 Corporation. Diesel (0#, $\eta_{25\text{ }^\circ\text{C}} = 5.43\text{ mPa}\cdot\text{s}$; $\rho_{25\text{ }^\circ\text{C}} = 0.825\text{ g}\cdot\text{cm}^{-3}$) was provided by
24 China National Petroleum Corporation. Bitumen samples and various dehydrated
25 crude oils were obtained from Liaohe, Xinan and Xijiang oilfields, China. All of these
26 experiment reagents were used without further purification.

27 II. Procedures for Preparation of HPAMAM and CHPAMAM

28 EDA (15.0 g, 0.25 mol) was dissolved in 50 mL of methanol containing MA (21.5
29 g, 0.25 mol) with magnetic stirring. The solution was stirred in an ice-water bath for
30 48 h, and most methanol was removed. Subsequently, the reaction system was kept in
31 an oil bath for 1.5 h at 60 °C to further process the residual methanol. The mixture
32 was reacted at 80 °C, 100 °C, 120 °C and 140 °C for 2 h, respectively, through a
33 rotary evaporator under vacuum to form macromolecules. HPAMAM was purified by
34 precipitating into ethyl ether and dried for 12 h at 50 °C in vacuo.



35
36 **Fig. S1** Preparation of hyperbranched poly(amido-amine) (HPAMAM) with MA and EDA as starting materials
37 and its functional product CHPAMAM

38 III. Preparation of oil-in-water (O/W) simulative emulsions

39 A series of oil-in-water emulsions were prepared: 10 % w/v diesel and 40 % w/v

40 diesel. For example, 100 g of diesel mixed with 0.18 g of Span 80 was added into a
41 1000 mL polypropylene beaker containing 1.82 g of Tween 80, and then, water was
42 added to reach the scale mark. Subsequently, the system was deeply stirred at 30000
43 $\text{r}\cdot\text{min}^{-1}$ for 15 min with a high-shear mechanical homogenizer (AF-B1, A-FIND,
44 China). The average droplet sizes of two kinds of emulsions measured by dynamic
45 light scattering (DLS) were less than 3 μm , which could ensure the adequate stability
46 of the emulsions during the experimental period.

47 **IV. Demulsification tests**

48 The demulsification effect was assessed by measuring the oil removal ratio of
49 emulsions and the water content of the upper phase. In each test, newly formulated
50 emulsions (50 mL) and the demulsifier solution (0.1 mL) with a given concentration
51 were mixed thoroughly by repeated oscillations in a 50 mL color-comparison tube.
52 The emulsions without any demulsifier were compared by applying the same
53 operation conditions as the blank experiment. Subsequently, the colorimetric tubes
54 were placed in a thermostatic water bath (DKZ-2, Shanghai Jinghong, China) to
55 maintain the specified temperature so as to investigate demulsification performance.
56 The residual oil in the lower phase was extracted with *n*-hexane and then its oil
57 content was analyzed by a UV-vis spectrophotometer (Shimadzu, UV-2450, Japan).
58 The oil content was converted into the oil removal ratio of emulsions to indicate the
59 demulsification effect as follows:

$$R = \frac{c_0 - c}{c_0} \times 100 \% \quad (1)$$

60 where R (%) is the oil removal ratio of emulsions, c_0 ($\text{mg}\cdot\text{L}^{-1}$) represents the initial oil

61 content of the emulsions, and c ($\text{mg}\cdot\text{L}^{-1}$) denotes the oil content during the process of
62 demulsification. The wavelength of the characteristic absorption peak of oil,
63 corresponding to c or c_0 , was at 337.8 nm. Furthermore, the water content of upper
64 phase was determined by Karl Fischer titration with a coulometric KF titrator (C20,
65 Mettler Toledo). To more intuitively monitor the effect of CHPAMAM on
66 demulsification process, the size of droplets in lower emulsion layer after different
67 settling time was observed by an optical microscope.

68 **V. Interfacial tension correlation**

69 The dynamic interface tension curves were fitted into a biexponential (four
70 parameter) decay equation to explore the ability of demulsifiers molecules to diffuse,
71 absorb and rearrange on the interface membrane:

$$\gamma = ae^{(-bt)} + ce^{(-dt)} \quad (2)$$

72 where γ is the function of oil-water interfacial tension with time, γ_0 is the initial
73 interfacial tension, b and d represent the decaying trend of oil-water interfacial tension
74 corresponding to the rapid attenuation in the initial stage and the subsequent slow
75 attenuation, respectively. All of the experimental measurements were repeated three
76 times and the average values were taken.

77 **VI. Interfacial film strength measurement**

78 The single-drop method was implemented to investigate the interfacial film
79 strength and the ability of demulsifier to damage the oil-water interfacial film. The
80 water phase containing the demulsifier and oil phase were placed in a constant
81 temperature water bath. Subsequently, the diesel droplets moved slowly in the water

82 phase to form O/W-type droplets. When emulsified oil droplets reached the stable oil-
83 water interfacial film, timing was triggered. The number of droplets in a single
84 experiment was 50, and the coalescence time of droplets was recorded. Based on the
85 Cockbain theory³⁴, the rupture rate constant k was calculated with the following
86 equation:

$$\ln \frac{N}{N_0} = kt + c \quad (3)$$

87 where N is the number of droplets at the moment t , N_0 represents the total number of
88 droplets involved in single experiment, and c denotes the regression factor.

89 The time required for half the number of experimental droplets to rupture is defined
90 as the half-life time of the droplets. The combination of half-life time ($t_{1/2}$), drainage
91 time (t_d), and rupture rate constant (k) can be used to evaluate interfacial film strength,
92 and the following relationship is obtained:

$$t_{1/2} = t_d + \frac{\ln 2}{k} \quad (4)$$

93 **VII. Interfacial rheology measurement**

94 Dilatational modulus (ε) is obtained from the ratio of the interfacial tension (γ)
95 response to the relative area (A) variation, as shown in the following equation:

$$\varepsilon = \frac{d\gamma}{d\ln A} \quad (5)$$

96 The dilatational modulus is divided into elastic modulus (ε') and viscous modulus (ε'').
97 The elastic modulus can effectively reflect the ability of the interfacial film to resist
98 deformation; the viscous modulus is used to predict the diffusion, adsorption and
99 rearrangement ability of the emulsion breaker molecules at the interface. Therefore,

100 dilatational modulus can be drawn as follows:

$$\varepsilon = \varepsilon' + i\varepsilon'' \quad (6)$$

$$\varepsilon'' = \omega\eta_d \quad (7)$$

101 where ω and η_d are defined as oscillation frequency of the interfacial film and
102 interfacial dilatational viscosity, respectively.

103 **VIII. Dissipative particle dynamics (DPD) method**

104 In the DPD simulation, N_m water molecules are typically coarse-grained into a bead.
105 Based on the previous research on the construction of oil-water simulation system, the
106 degree of coarse-grained is set to $N_m = 3$, indicating that one DPD water bead
107 corresponds to three water molecules in the simulation system of this work. The
108 scales of length (R_c), mass (m), and time (τ) can be evaluated in terms of the coarse
109 graining:

$$R_c = 3.107(\rho N_m)^{1/3} \text{ \AA} \quad (8)$$

$$m = N_m \cdot m_{\text{water}} \text{ amu} \quad (9)$$

$$\tau = (1.41 \pm 0.1)N_m^{5/3} \text{ ps} \quad (10)$$

110 where the reduced density $\rho = 3$, which denotes the number of beads in a cubic
111 volume of radius R_c is 3; m_{water} is the mass of a water molecule. The above three
112 scales are calculated as $R_c = 6.46 \text{ \AA}$, $m = 54 \text{ amu}$, $\tau = 8.8 \text{ ps}$.

113 The reasonable calculation of the interaction parameters between different
114 structural units is the most critical in DPD simulation to construct the force field of
115 the whole coarse-grained model and explore the motion state of each particle in the
116 system from the mesoscopic level. The DPD theory is correlated with the Flory -

117 Huggins theory, and the DPD conservative force parameters (a_{ij}) are further derived
118 from the Flory-Huggins parameters (χ_{ij}), thus achieving the integration of abstract
119 models and real chemical components, the empirical correlation as follows:

$$a_{ij} \approx a_{ii} + 3.27\chi_{ij}(\rho = 3) \quad (11)$$

120 where a_{ii} is the repulsive force between homogeneous beads, and ρ is the density of
121 the number of particles in the system. The density ρ of coarse-grained beads is set to 3,
122 therefore the initial a_{ii} is 25, and a_{ij} is 78 in this emulsion system. The parameters χ_{ij} at
123 different temperatures can be deduced by calculating the solubility parameters of
124 beads i and j in the system:

$$\chi_{ij} = \frac{v_{ij}}{RT}(\delta_i - \delta_j)^2 \quad (12)$$

125 where v_{ij} is the average molar volume of beads i and j , R is the ideal gas constant, δ_i
126 and δ_j are the Hansen solubility parameters of each bead at temperature T . For
127 macromolecular systems where the solubility parameters are difficult to be measured
128 experimentally, the solubility parameters of individual beads in this model are further
129 obtained by Cohesion Energy Density (CED) calculation, as shown in the following
130 equation:

$$\delta_i = \sqrt{\frac{E_{\text{coh}}}{V_i^0}} = \sqrt{\frac{\Delta_{\text{vap}}H_m - RT}{V_i^0}} \quad (13)$$

131 where E_{coh} , V_i^0 and $\Delta_{\text{vap}}H_m$ are the cohesive energy, volume and enthalpy of
132 vaporization of component i , respectively. The calculations are performed with the
133 Forcite module in Materials Studio software.

134

135

136

137

Table S1 Volume (v) of coarse-grained beads at 303.15 K/ \AA^3

303.15K	A ₂	A ₃	A ₄	A ₆	R ₂	R ₃	R ₄	O ₁	O ₂	S	N ₁	N ₂	W	PAM	P ₁	P ₂	P ₃	P ₄
A ₂	58.10																	
A ₃	65.60	73.10																
A ₄	73.85	81.35	89.60															
A ₆	73.75	81.25	89.50	89.40														
R ₂	56.65	64.15	72.40	72.30	55.20													
R ₃	66.87	74.37	82.62	82.52	65.42	75.62												
R ₄	76.30	83.80	92.05	91.95	74.85	85.05	94.50											
O ₁	72.95	80.45	88.70	88.60	71.50	81.70	91.15	87.80										
O ₂	58.45	65.95	74.20	74.10	57.00	67.20	76.65	73.30	58.80									
S	65.60	73.10	81.35	81.25	64.15	74.35	83.80	80.45	65.95	73.10								
N ₁	71.40	78.90	87.15	87.05	69.95	80.15	89.60	86.25	71.75	78.90	84.70							
N ₂	61.65	69.15	77.40	77.30	60.20	70.40	79.85	76.50	62.00	69.15	74.95	65.20						
W	38.05	45.55	53.80	53.70	36.60	46.80	56.25	52.90	38.40	45.55	51.35	41.60	18.00					
PAM	59.79	67.29	75.54	75.44	58.34	68.54	77.99	74.64	60.14	67.29	73.09	63.34	39.74	61.49				
P ₁	58.20	65.70	73.95	73.85	56.75	66.95	76.40	73.05	58.55	65.70	71.50	61.75	38.15	59.90	58.30			
P ₂	71.00	78.50	86.75	86.65	69.55	79.75	89.20	85.85	71.35	78.50	84.30	74.55	50.95	72.70	71.10	83.90		
P ₃	53.40	60.90	69.15	69.05	51.95	62.15	71.60	68.25	53.75	60.90	66.70	56.95	33.35	55.10	53.50	66.30	48.70	
P ₄	95.80	103.30	111.55	111.45	94.35	104.55	114.00	110.65	96.15	103.30	109.10	99.35	75.75	97.50	95.90	108.70	91.10	133.50

138

Table S2 Volume (v) of coarse-grained beads at 318.15 K/ \AA^3

318.15K	A ₂	A ₃	A ₄	A ₆	R ₂	R ₃	R ₄	O ₁	O ₂	S	N ₁	N ₂	W	PAM	P ₁	P ₂	P ₃	P ₄
A ₂	58.10																	
A ₃	65.60	73.10																
A ₄	73.85	81.35	89.60															
A ₆	73.75	81.25	89.50	89.40														
R ₂	56.65	64.15	72.40	72.30	55.20													
R ₃	66.87	74.37	82.62	82.52	65.42	75.62												
R ₄	76.30	83.80	92.05	91.95	74.85	85.05	94.50											
O ₁	72.95	80.45	88.70	88.60	71.50	81.70	91.15	87.80										
O ₂	58.45	65.95	74.20	74.10	57.00	67.20	76.65	73.30	58.80									
S	65.60	73.10	81.35	81.25	64.15	74.35	83.80	80.45	65.95	73.10								
N ₁	71.40	78.90	87.15	87.05	69.95	80.15	89.60	86.25	71.75	78.90	84.70							
N ₂	61.65	69.15	77.40	77.30	60.20	70.40	79.85	76.50	62.00	69.15	74.95	65.20						
W	38.05	45.55	53.80	53.70	36.60	46.80	56.25	52.90	38.40	45.55	51.35	41.60	18.00					
PAM	59.79	67.29	75.54	75.44	58.34	68.54	77.99	74.64	60.14	67.29	73.09	63.34	39.74	61.49				
P ₁	58.20	65.70	73.95	73.85	56.75	66.95	76.40	73.05	58.55	65.70	71.50	61.75	38.15	59.90	58.30			

P₂	71.00	78.50	86.75	86.65	69.55	79.75	89.20	85.85	71.35	78.50	84.30	74.55	50.95	72.70	71.10	83.90		
P₃	53.40	60.90	69.15	69.05	51.95	62.15	71.60	68.25	53.75	60.90	66.70	56.95	33.35	55.10	53.50	66.30	48.70	
P₄	95.80	103.30	111.55	111.45	94.35	104.55	114.00	110.65	96.15	103.30	109.10	99.35	75.75	97.50	95.90	108.70	91.10	133.50

139

140

141

Table S3 Volume (v) of coarse-grained beads at 333.15 K/ Å³

333.15K	A₂	A₃	A₄	A₆	R₂	R₃	R₄	O₁	O₂	S	N₁	N₂	W	PAM	P₁	P₂	P₃	P₄
A₂	58.10																	
A₃	65.60	73.10																
A₄	73.85	81.35	89.60															
A₆	73.75	81.25	89.50	89.40														
R₂	56.65	64.15	72.40	72.30	55.20													
R₃	66.87	74.37	82.62	82.52	65.42	75.62												
R₄	76.30	83.80	92.05	91.95	74.85	85.05	94.50											
O₁	72.95	80.45	88.70	88.60	71.50	81.70	91.15	87.80										
O₂	58.45	65.95	74.20	74.10	57.00	67.20	76.65	73.30	58.80									
S	65.60	73.10	81.35	81.25	64.15	74.35	83.80	80.45	65.95	73.10								
N₁	71.40	78.90	87.15	87.05	69.95	80.15	89.60	86.25	71.75	78.90	84.70							
N₂	61.65	69.15	77.40	77.30	60.20	70.40	79.85	76.50	62.00	69.15	74.95	65.20						
W	38.05	45.55	53.80	53.70	36.60	46.80	56.25	52.90	38.40	45.55	51.35	41.60	18.00					
PAM	59.79	67.29	75.54	75.44	58.34	68.54	77.99	74.64	60.14	67.29	73.09	63.34	39.74	61.49				
P₁	58.20	65.70	73.95	73.85	56.75	66.95	76.40	73.05	58.55	65.70	71.50	61.75	38.15	59.90	58.30			
P₂	71.00	78.50	86.75	86.65	69.55	79.75	89.20	85.85	71.35	78.50	84.30	74.55	50.95	72.70	71.10	83.90		
P₃	53.40	60.90	69.15	69.05	51.95	62.15	71.60	68.25	53.75	60.90	66.70	56.95	33.35	55.10	53.50	66.30	48.70	
P₄	95.80	103.30	111.55	111.45	94.35	104.55	114.00	110.65	96.15	103.30	109.10	99.35	75.75	97.50	95.90	108.70	91.10	133.50

142

Table S4 Solubility parameter (δ) of coarse-grained beads at 303.15 K/ MPa^{1/2}

303.15K	A₂	A₃	A₄	A₆	R₂	R₃	R₄	O₁	O₂	S	N₁	N₂	W	PAM	P₁	P₂	P₃	P₄
A₂	0.00																	
A₃	6.02	0.00																
A₄	11.99	1.02	0.00															
A₆	17.91	3.16	0.59	0.00														
R₂	0.38	9.42	16.63	23.50	0.00													
R₃	0.03	5.15	10.75	16.38	0.64	0.00												
R₄	0.71	2.59	6.86	11.48	2.13	0.44	0.00											
O₁	54.33	24.18	15.27	9.85	63.79	51.64	42.59	0.00										
O₂	72.89	37.01	25.75	18.53	83.78	69.77	59.18	1.36	0.00									
S	24.78	6.37	2.29	0.56	31.28	22.97	17.08	5.73	12.67	0.00								
N₁	42.47	16.51	9.33	5.22	50.88	40.10	32.18	0.73	4.08	2.37	0.00							
N₂	20.04	4.09	1.03	0.06	25.93	18.42	13.19	8.38	16.49	0.25	4.16	0.00						
W	1053.33	900.09	840.56	796.52	1093.68	1041.38	999.23	629.22	572.05	755.01	672.77	782.79	0.00					
PAM	165.76	108.61	88.59	74.69	182.00	161.04	144.73	30.30	18.81	62.37	40.42	70.53	383.38	0.00				

P₁	3.72	0.27	2.35	5.30	6.48	3.05	1.18	29.60	43.66	9.29	21.04	6.49	931.78	119.79	0.00				
P₂	145.49	92.32	73.95	61.30	160.73	141.07	125.84	22.01	12.42	50.19	30.75	57.54	415.87	0.66	102.66	0.00			
P₃	91.84	50.84	37.46	28.63	104.02	88.34	76.37	4.90	1.09	21.21	9.40	26.08	523.11	10.83	58.58	6.14	0.00		
P₄	50.92	21.92	13.49	8.43	60.08	48.32	39.58	0.06	1.97	4.66	0.38	7.07	641.08	32.94	27.10	24.27	5.99	0.00	

143

144

145

Table S5 Solubility parameter (δ) of coarse-grained beads at 318.15 K/ MPa^{1/2}

318.15K	A₂	A₃	A₄	A₆	R₂	R₃	R₄	O₁	O₂	S	N₁	N₂	W	PAM	P₁	P₂	P₃	P₄	
A₂	0.00																		
A₃	6.64	0.00																	
A₄	13.81	1.30	0.00																
A₆	20.23	3.69	0.61	0.00															
R₂	0.22	9.28	17.52	24.67	0.00														
R₃	0.33	4.01	9.87	15.39	1.09	0.00													
R₄	1.17	2.23	6.94	11.66	2.41	0.26	0.00												
O₁	60.94	27.35	16.72	10.95	68.48	52.30	45.20	0.00											
O₂	75.19	37.14	24.54	17.41	83.53	65.55	57.57	0.75	0.00										
S	27.10	6.91	2.22	0.50	32.20	21.45	17.00	6.76	12.01	0.00									
N₁	43.86	16.37	8.44	4.51	50.28	36.57	30.68	1.40	4.20	2.01	0.00								
N₂	20.84	3.95	0.72	0.00	25.33	15.92	12.12	10.51	16.86	0.41	4.23	0.00							
W	1034.02	874.93	808.78	764.98	1064.37	997.38	965.53	592.91	551.55	726.31	651.97	761.29	0.00						
PAM	168.52	108.26	85.83	71.97	180.91	153.93	141.57	26.78	18.58	60.46	40.44	70.85	367.66	0.00					
P₁	4.76	0.16	2.36	5.37	7.02	2.58	1.21	31.64	42.12	9.15	19.72	5.68	898.49	116.65	0.00				
P₂	152.63	95.60	74.60	61.72	164.42	138.75	127.04	20.68	13.57	51.10	32.85	60.68	392.12	0.39	103.49	0.00			
P₃	92.57	49.62	34.86	26.25	101.81	81.84	72.90	3.29	0.90	19.49	8.99	25.57	507.82	11.29	55.35	7.47	0.00		
P₄	55.07	23.47	13.72	8.55	62.25	46.87	40.17	0.15	1.56	4.91	0.64	8.16	611.82	30.92	27.46	24.33	4.84	0.00	

146

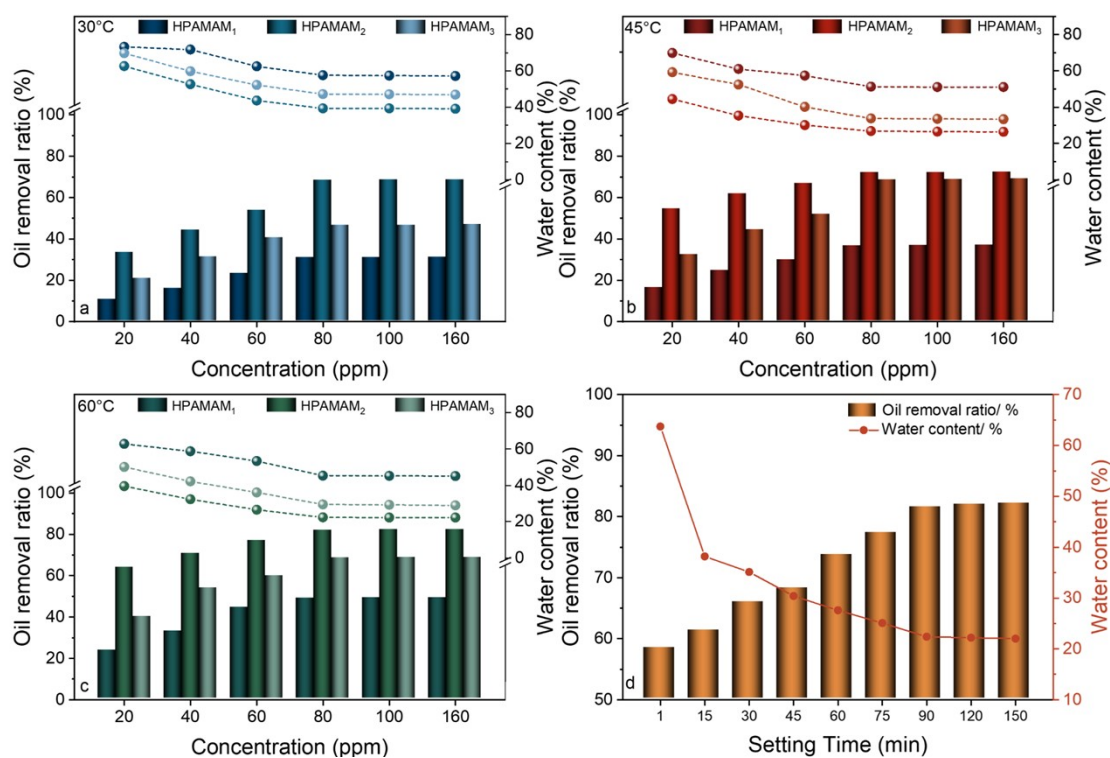
Table S6 Solubility parameter (δ) of coarse-grained beads at 333.15 K/ MPa^{1/2}

333.15K	A₂	A₃	A₄	A₆	R₂	R₃	R₄	O₁	O₂	S	N₁	N₂	W	PAM	P₁	P₂	P₃	P₄	
A₂	0.00																		
A₃	7.03	0.00																	
A₄	15.94	1.80	0.00																
A₆	23.68	4.91	0.76	0.00															
R₂	0.02	6.26	14.77	22.24	0.00														
R₃	2.02	1.52	6.62	11.87	1.61	0.00													
R₄	2.81	0.95	5.37	10.18	2.33	0.07	0.00												
O₁	64.05	28.64	16.08	9.84	61.67	43.34	40.03	0.00											
O₂	73.98	35.40	21.23	13.95	71.42	51.57	47.96	0.36	0.00										
S	31.38	8.71	2.59	0.54	29.72	17.49	15.41	5.76	8.99	0.00									
N₁	52.01	20.80	10.36	5.50	49.87	33.55	30.65	0.63	1.93	2.59	0.00								
N₂	23.15	4.67	0.67	0.00	21.72	11.50	9.83	10.19	14.36	0.63	5.76	0.00							
W	1093.96	925.62	845.76	795.75	1084.06	1002.04	985.90	628.61	598.98	754.77	668.89	798.85	0.00						

Table S14 Characterization of synthesized HPAMAM and CHPAMAM samples.

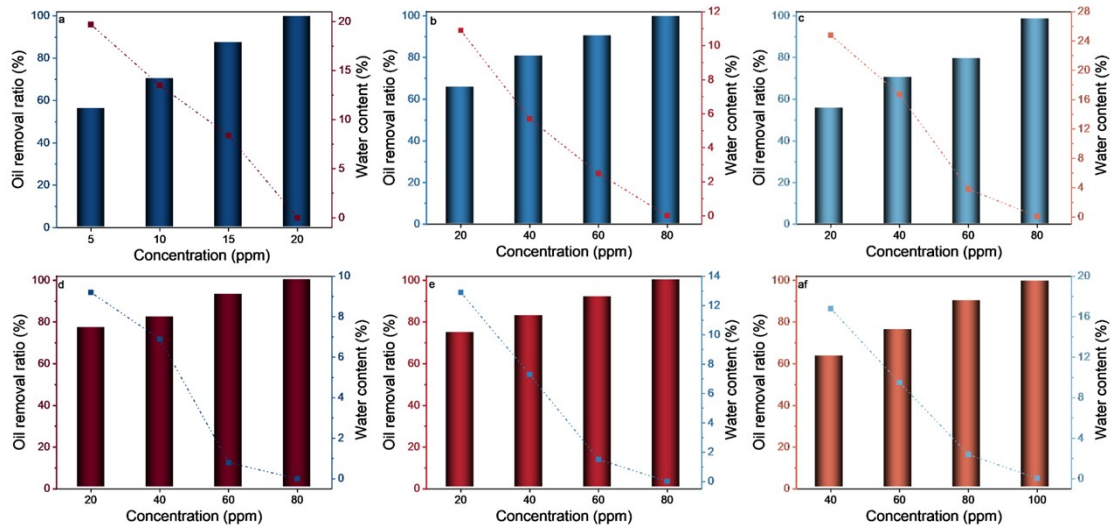
Polymer	RNH ₂	R ₂ NH	R ₃ N	HLB	Size (nm)
HPAMAM ₁	27	50	24	13.15	3.97
HPAMAM ₂	52	121	36	14.26	4.46
HPAMAM ₃	106	218	94	14.51	5.06
CHPAMAM _{1-15%}	17	44	24	8.13	4.12
CHPAMAM _{2-5%}	44	118	36	12.14	4.86
CHPAMAM _{2-10%}	34	117	36	10.49	5.11
CHPAMAM _{2-15%}	31	111	36	9.91	5.37
CHPAMAM _{2-20%}	22	108	36	8.31	5.78
CHPAMAM _{3-15%}	65	196	94	9.06	6.01

166 X. The evaluation experiment of HPAMAM demulsification effect



168 Fig. S3 Effects of demulsifier concentration and operation temperature on the demulsification
 169 performance (column: oil removal ratio of emulsions and line+symbol: water content of oil phase) with
 170 CHPAMAM as demulsifiers after 40 min at different temperatures ranging from 30 °C to 60 °C for the
 171 emulsions with oil-water ratios of 1:9.

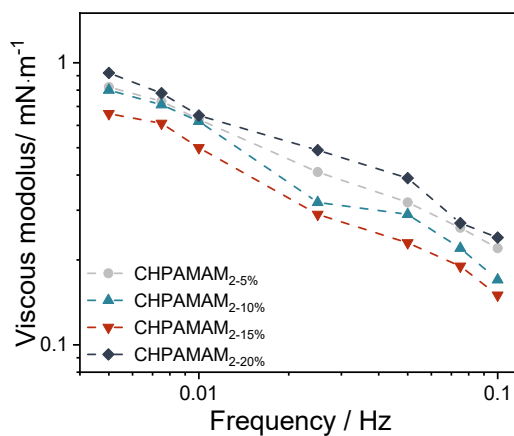
172 XI. The demulsification performance of CHPAMAM in different emulsions



173

174 **Fig. S4** Demulsification performance of CHPAMAM demulsifier on (a) crude oil/ water emulsions with
 175 50 % crude oil after setting for 30 min, (b) water/ crude oil emulsions with 10 % water after setting for
 176 40 min, (c) water/ bitumen emulsions with 5.0 % water after setting for 30 min, (d) light crude oil/
 177 water emulsions with 40 % light crude oil after setting for 30 min, (e) crude oil/ water emulsions with
 178 1.0 % crude oil after setting for 10 min, (f) water/ crude oil emulsions with 50 % crude oil after setting
 179 for 20 min.

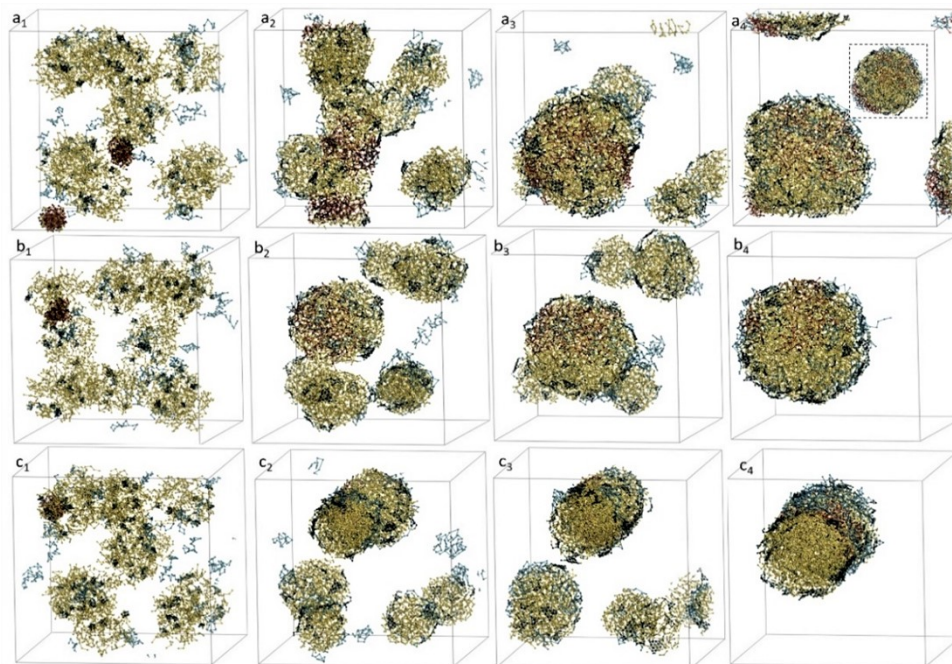
180 **XII. The tendency of the viscous modulus with CHPAMAM at various oscillation**
 181 **frequencies**



182

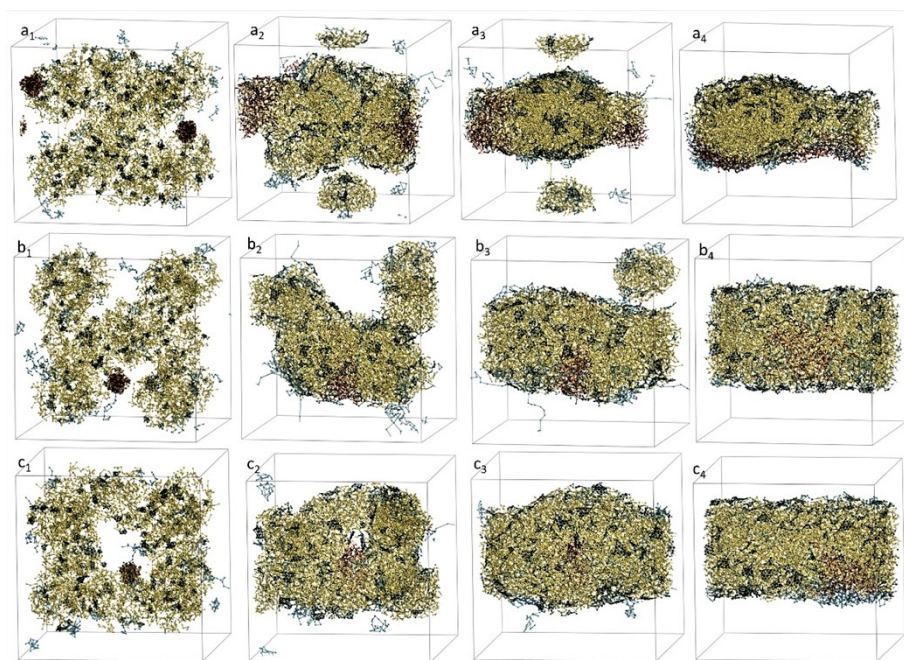
183 **Fig. S5** Effect of the oscillating frequency on viscous modulus of oil-water interface containing Span 80 and
 184 Tween 80 with 80 ppm CHPAMAM demulsifiers.

185 **XIII. Simulation of dissipative particle dynamics**



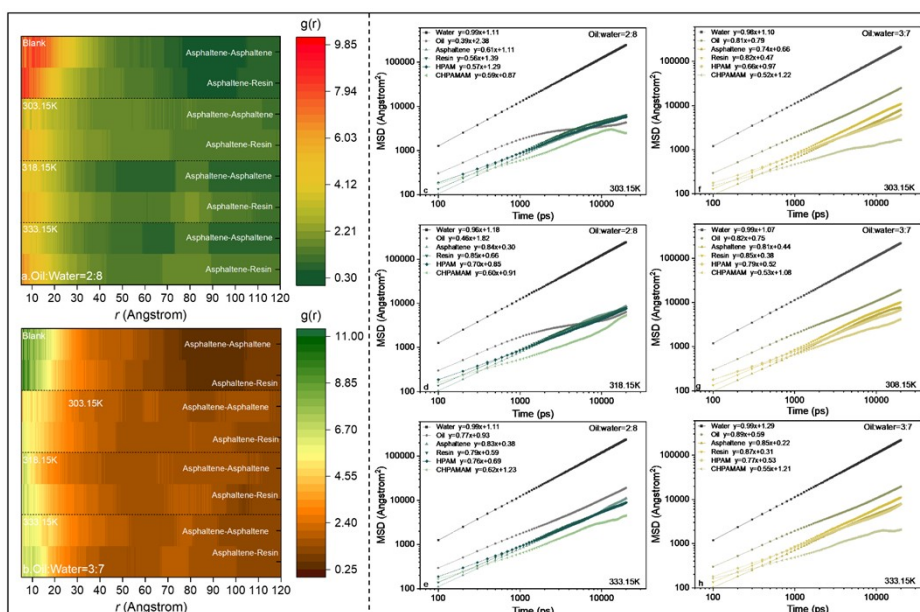
186

187 **Fig.S6** Effect of temperature on the demulsification process for the emulsions of oil-water ratios 2:8 with
 188 CHPAMAM during the DPD simulation (Model basic parameters: temperature is (a) 303.15K, (b) 318.15K, or (c)
 189 333.15K, and CHPAMAM concentration is 80 ppm) at different time steps: (a₁-c₁) 5×10^4 steps; (a₂-c₂) 20
 190 $\times 10^4$ steps; (a₃-c₃) 160×10^4 steps; (a₄-c₄) 240×10^4 steps.



191

192 **Fig.S7** Effect of temperature on the demulsification process for the emulsions of oil-water ratios 3:7 with
 193 CHPAMAM during the DPD simulation (Model basic parameters: Temperature is (a) 303.15K, (b) 318.15K, (c)
 194 333.15K, respectively, and CHPAMAM concentration is 80 ppm) at different time steps: (a₁-c₁) 5×10^4 steps; (a₂-c₂)
 195 20×10^4 steps; (a₃-c₃) 160×10^4 steps; (a₄-c₄) 240×10^4 steps.



196

197 **Fig.S8** Radial distribution functions of asphaltene and asphaltene, asphaltene and resin in emulsions with oil-water
 198 ratios (a) 2:8 and (b) 3:7 after adding 80 ppm CHPAMAM at different temperatures. Mean square displacements
 199 of each component in emulsions with oil-water ratios (c-e) 1:9 and (f-h) 4:6 after adding 80 ppm CHPAMAM at
 200 different temperatures.

201 XIV. Components of crude oil produced emulsions

202 **Table S15** Characteristics of produced emulsions from two China oilfields

Parameter	value	Parameter	value
Xinan Oilfield			
Oil content	13.4 %	Salinity	4315.5 mg L ⁻¹
pH	8.8	Mg ²⁺	10.3 mg L ⁻¹
Density at 293 K	0.90 g cm ⁻³	Ca ²⁺	34.5 mg L ⁻¹
Viscosity at 329 K	89.2 mPa s	K ⁺ + Na ⁺	2493.1 mg L ⁻¹
Asphaltene	2.7 %	Cl ⁻	2034.2 mg L ⁻¹
Resin	19.4 %	HCO ₃ ⁻	1469.4 mg L ⁻¹
Xinjiang Oilfield			
Oil content	38.7 %	Salinity	10451.8 mg L ⁻¹
pH	10.7	Mg ²⁺	15.3 mg L ⁻¹
Density at 293 K	0.98 g cm ⁻³	Ca ²⁺	29.7 mg L ⁻¹
Viscosity at 329 K	6250.3 mPa s	K ⁺ + Na ⁺	5128.7 mg L ⁻¹
Asphaltene	10.6 %	Cl ⁻	4962.6 mg L ⁻¹
Resin	24.3 %	HCO ₃ ⁻	1531.2 mg L ⁻¹

203